Supplemental material

Engineering second-generation TCR-T cells by site-specific integration of TRAF-binding motifs into the *CD247* locus

This PDF file includes:

Supplemental figures 1 to 11, and table1.

Lah S, *et al. J Immunother Cancer* 2023; 11:e005519. doi: 10.1136/jitc-2022-005519

Contents

32 Supplemental reference.

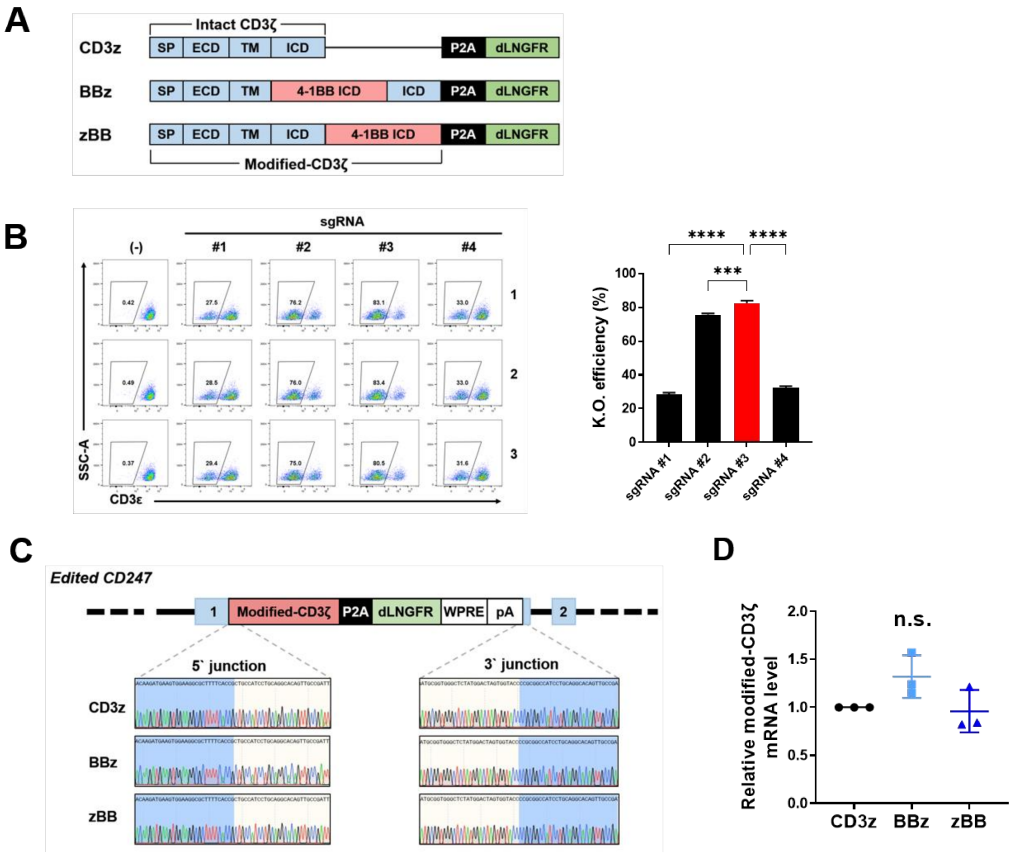

Supplemental figure 1. Site-specific integration of modified-CD3ζ constructs into the *CD247* locus.

(A) Gene schematics of the modified-CD3ζ constructs. (B) Screening sequence of sgRNAs targeting *CD247*. (C) In-Out PCR for targeted integration of modified-CD3ζ at *CD247* locus. (D) mRNA expression level of modified-CD3ζ in CD3z-, BBz-, and zBB-KI T cells. P-values (***P < 0.001 and ****P < 0.0001) were determined using one-way ANOVA, with Tukey's multiple comparisons *post-hoc* test (B, D). Data have been presented as mean ± SEM. n.s., not significant; SP, signal peptide; ECD, extracellular domain; TM, transmembrane; ICD, intracellular domain.

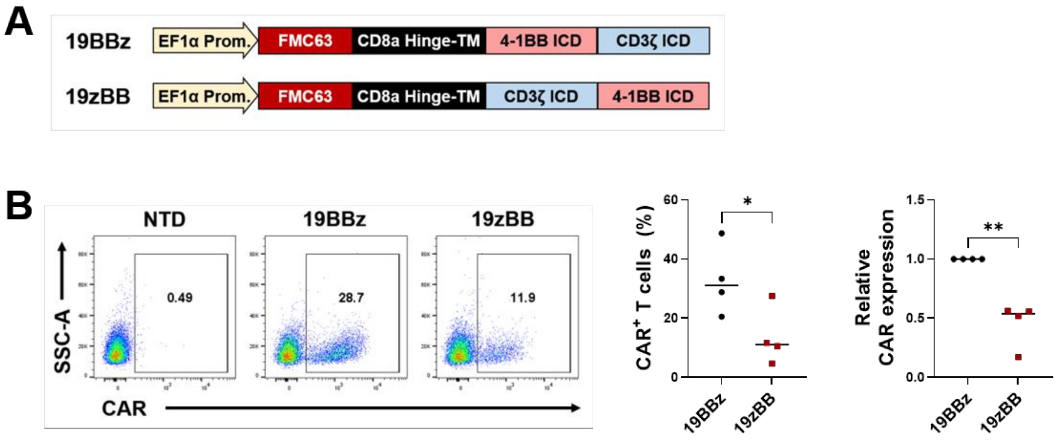

Supplemental figure 2. Comparison of the expression levels of the two distinct CAR constructs, 19BBz and 19zBB.

(A) Gene schematics of CAR constructs on lentiviral vectors that were used to generate 19BBz and 19zBB CAR T cells. CD19-specific CAR used the single-chain variable fragments from the FMC63 antibody. Hinge/transmembrane and intracellular domains are indicated. (B) Representative flow cytometric analysis of the proportion of cells positive for CAR in primary human T cells (left). Percent (middle) and relative mean fluorescence intensity (MFI; right) of the indicated CARs. Two-tailed student's *t*-test was used to determine significance (*P < 0.05 and **P < 0.01). Data have been presented as mean ± SEM.

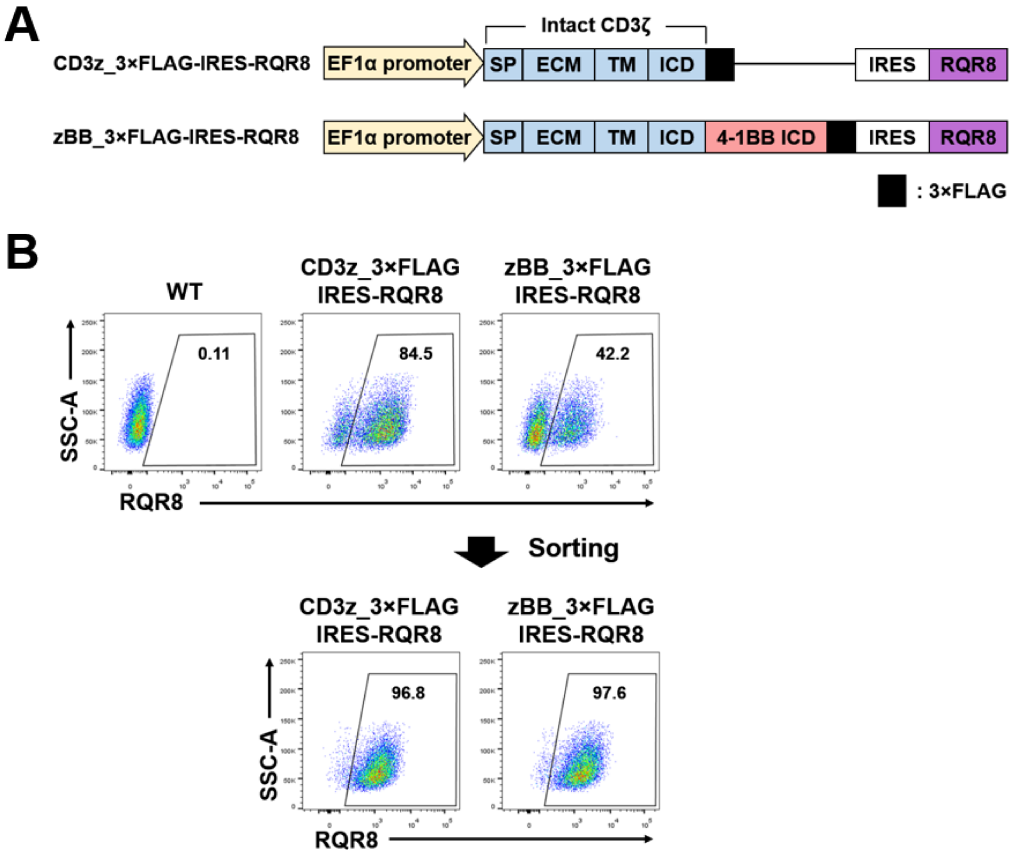

Supplemental figure 3. Generation of zBB_3×FLAG transduced Jurkat cells for co-immunoprecipitation.

(A) Gene schematics of CD3z_3×FLAG and zBB_3×FLAG in lentiviral vectors carrying a bicistronic RQR8 reporter.[1] (B) Transduction (top) and sorting (bottom) efficiency of CD3z_3×FLAG- and zBB_3×FLAG-transduced CD3ζ-KO Jurkat cells. $RQR8^+$ Jurkat cells were isolated using anti-CD34-PE monoclonal antibodies and PE^+ MACS beads. SP, signal peptide; ECD, extracellular domain; TM, transmembrane; ICD, intracellular domain.

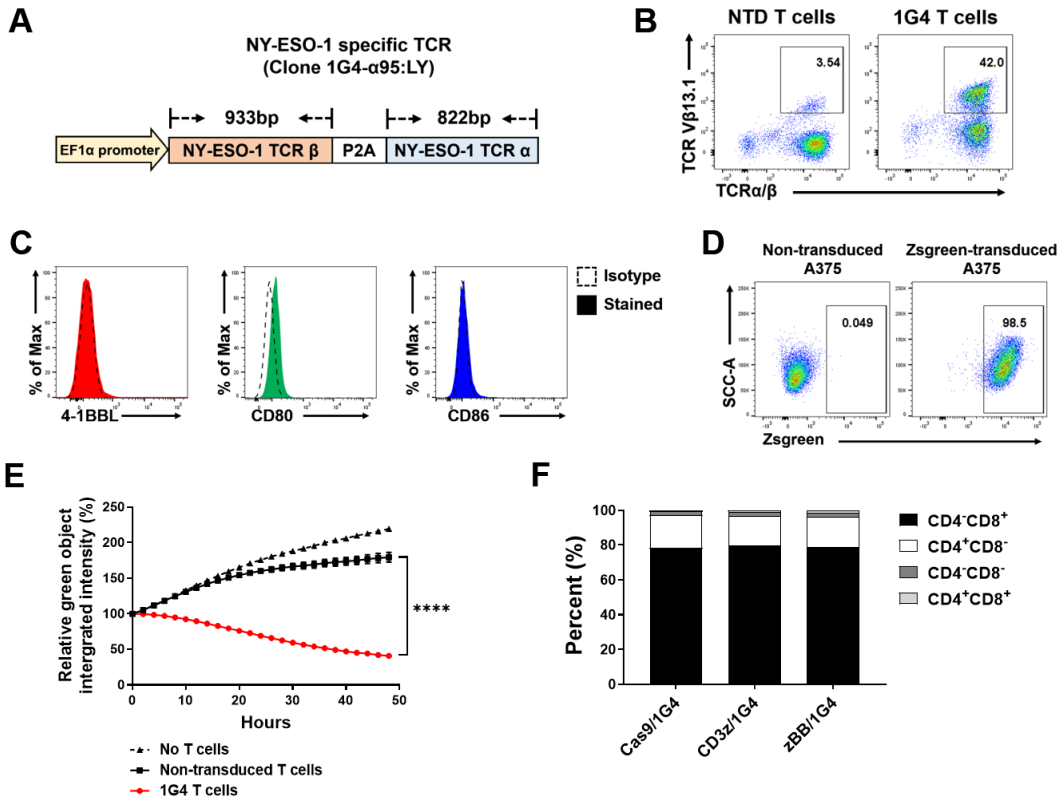

Supplemental figure 4. Generation of NY-ESO-1-specific TCR-T cells and evaluation of their cytolytic potential.

(A) Schematic diagram of NY-ESO-1-specific TCR (clone 1G4-α95:LY). A P2A peptide enables co-expression of TCRβ and TCRα under the EF1α promoter. (B) Percentage of TCR Vβ13.1 in NTD and 1G4 T cells. (C) Expression of co-stimulatory ligands, CD80, CD86, and 4-1BBL, in A375 cells. (D) Proportion of Zsgreen in non (left panel)- and Zsgreen (right panel)-transduced A375 cells. (E) *In vitro* cytotoxicity of 1G4 TCR-T cells against the NY-ESO-1-expressing melanoma cell line A375. 1G4 TCR-T cells were incubated with Zsgreen-expressing A375 at an effector:target (E:T) ratio of 1:1. Green fluorescence intensity was measured using the IncuCyte™ S3 live-cell imaging system. (F) CD4/CD8 compositions

(ratios) of Cas9/1G4, CD3z/1G4, and zBB/1G4 T cells. P-values (****P < 0.0001) were determined using two-way ANOVA, with Tukey's multiple comparisons *post-hoc* test (E). NTD, non-transduced.

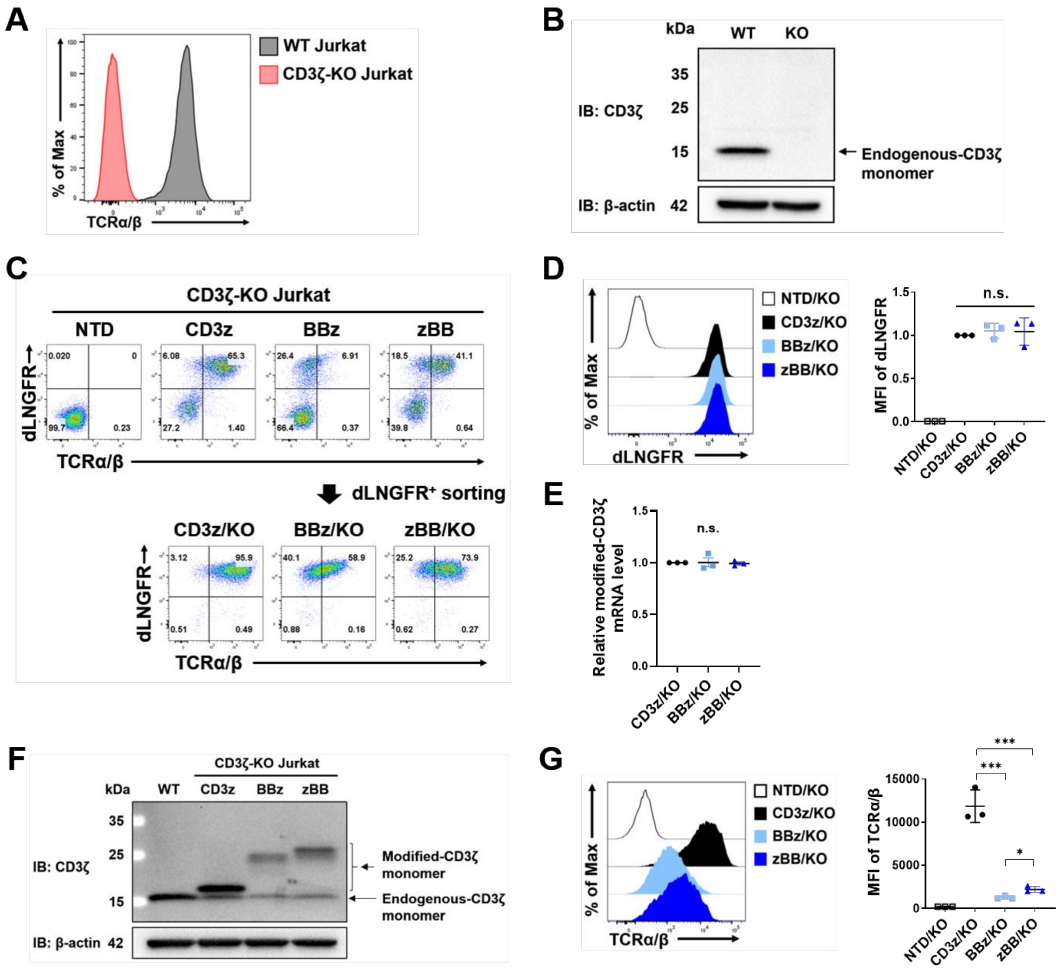

Supplemental figure 5. Generation of BBz- or zBB-transduced CD3ζ-KO Jurkat cells.

(A) Representative histograms of TCRα/β in WT (gray shaded histogram) and CD3ζ-KO (red shaded histogram) Jurkat cells. (B) Western blot analysis of endogenous-CD3ζ in WT and CD3ζ-KO Jurkat cells. β-actin was used as a loading control. Representative results from one of three repeated experiments are shown. (C) Representative flow cytometric analysis showing the proportion of dLNGFR- and TCRα/β-positive cells in CD3ζ-KO Jurkat cells expressing CD3z, BBz, or zBB, which indicate cells before (top) and after (bottom) sorting. (D) Representative histogram (left) and MFI (right) of dLNGFR in CD3z-, BBz-, and zBB-

transduced CD3ζ-KO Jurkat cells from (C, bottom). (E) mRNA expression level of modified-CD3ζ in CD3z-, BBz-, or zBB-transduced CD3ζ-KO Jurkat cells. (F) Western blot analysis of modified-CD3ζ in WT and CD3ζ-KO Jurkat cells. β-actin was used as a loading control. Results are representative of one of two repeated experiments. (G) Representative histogram (left) and MFI (right) of the TCRα/β complex in CD3z-, BBz-, and zBB-transduced CD3ζ-KO Jurkat cells from (C, bottom). P-values (*P < 0.05 and ***P < 0.001) were determined using one-way ANOVA, with Tukey's multiple comparisons *post-hoc* test (D, E, and G). Data have been presented as mean ± SEM. n.s., not significant.

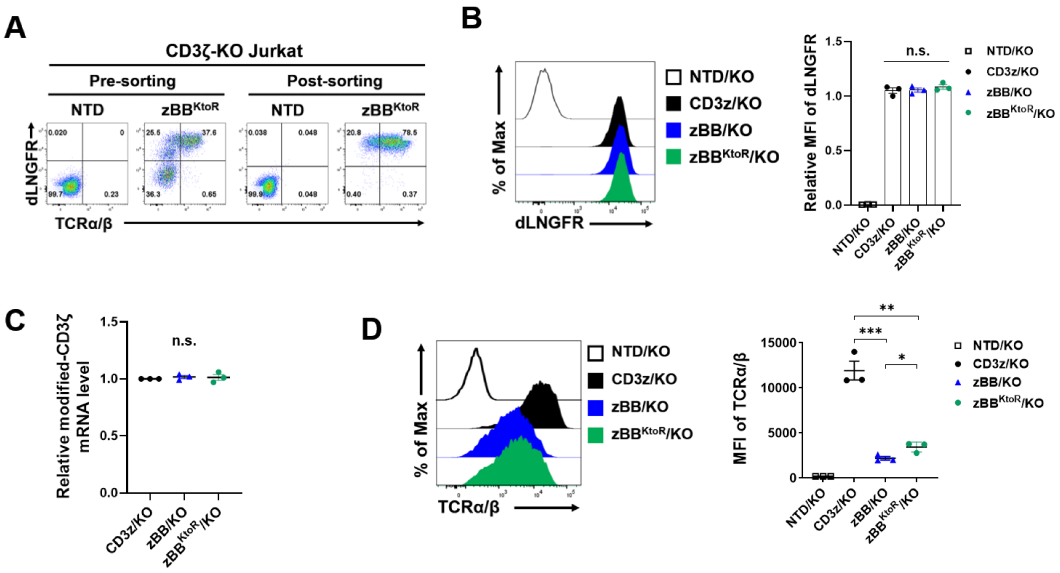

Supplemental figure. 6 Analysis of CD3ζ-KO Jurkat cells expressing zBB^{KtoR}.

(A) Representative flow cytometric analysis showing the proportion of dLNGFR- and TCRα/β-positive cells in zBB^{KtoR}-transduced CD3ζ-KO Jurkat cells. (B) Representative histogram (left) and MFI (right) of dLNGFR in zBB^{KtoR}-transduced CD3ζ-KO Jurkat cells. (C) mRNA abundance of modified-CD3ζ in zBB^{KtoR}-transduced CD3ζ-KO Jurkat cells. (D) Representative histogram (left) and MFI (right) of TCRα/β in zBB^{KtoR}-transduced CD3ζ-KO Jurkat cells. P-values (*P < 0.05, **P < 0.01, and ***P < 0.001) were determined using one-way ANOVA, with Tukey's multiple *post-hoc* comparisons test (B-D). Data have been presented as mean ± SEM. n.s., not significant.

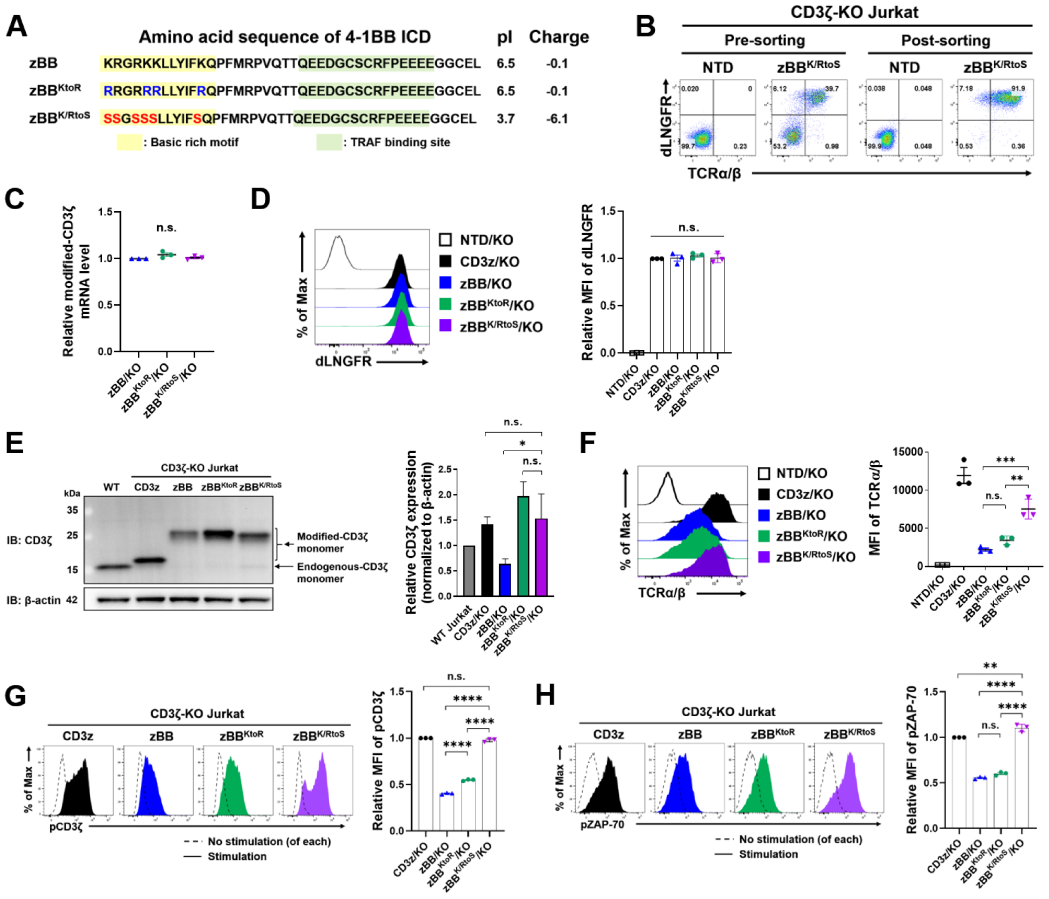

Supplemental figure 7. The restoration of TCR signaling by substituting serine for the arginine and lysine in the BRM.

(A) Amino acid sequence and isoelectric point of zBB$^{K/RtoS}$. (B) Representative flow cytometric analysis of the proportion of cells positive for dLNGFR and TCRα/β in zBB$^{K/RtoS}$-expressing CD3ζ-KO Jurkat cells. (C) mRNA abundance level of modified-CD3ζ in zBB$^{K/RtoS}$-transduced CD3ζ-KO Jurkat cells. (D) Representative histogram (left) and MFI (right) of dLNGFR in zBB$^{K/RtoS}$-transduced CD3ζ-KO Jurkat cells. (E) Western blot analysis of modified-CD3ζ in CD3z-, zBB-, zBB^{KtoR}-, and zBB$^{K/RtoS}$-transduced CD3ζ-KO Jurkat cells (left). β-actin was used as a loading control. Results are representative of one of three

repeated experiments. Quantification of the relative abundances of modified-CD3ζ, normalized to β-actin protein (right). (F) Representative histogram (left) and MFI (right) of TCRα/β in zBB$^{K/RtoS}$-transduced CD3ζ-KO Jurkat cells. (G) Phosphorylation of CD3ζ in zBB$^{K/RtoS}$-transduced CD3ζ-KO Jurkat cells. (H) Phosphorylation of ZAP-70 in zBB$^{K/RtoS}$-transduced CD3ζ-KO Jurkat cells. P-values (*P < 0.05, **P < 0.01, ***P < 0.001, and ****P < 0.0001) were determined using one-way ANOVA, with Tukey's multiple comparisons *post-hoc* test (C-H). Data have been presented as mean ± SEM. n.s., not significant.

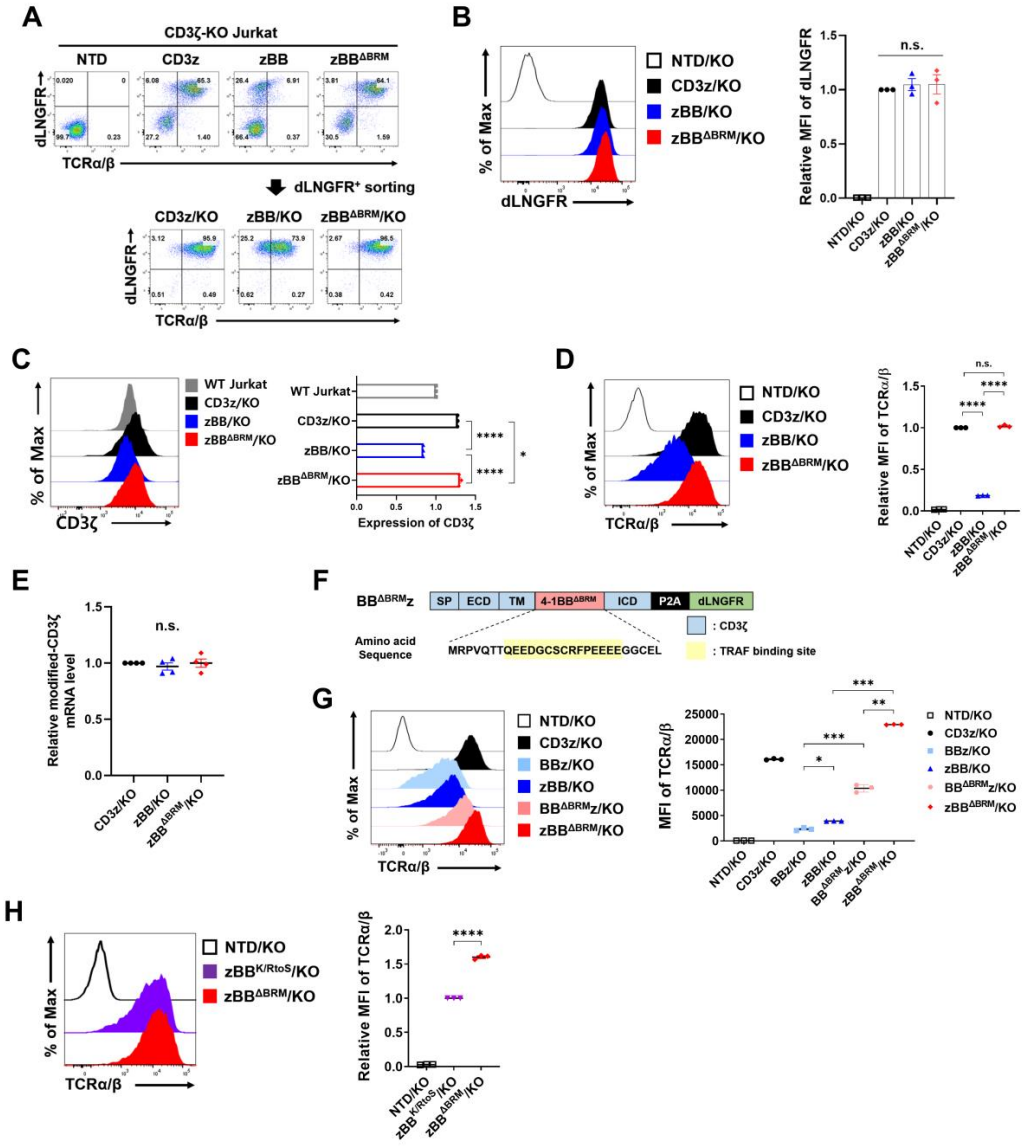

120

121 **Supplemental figure 8. Generation of zBB$^{\Delta BRM}$-transduced CD3ζ-KO Jurkat cells.**

122 (A) Representative flow cytometric analysis of the proportion of cells positive for dLNGFR
123 and TCRα/β in zBB$^{\Delta BRM}$-expressing CD3ζ-KO Jurkat cells showing the indicated cells before
124 (top) and after (bottom) sorting. (B) Representative histogram (left) and MFI (right) of
125 dLNGFR in zBB$^{\Delta BRM}$-transduced CD3ζ-KO Jurkat cells from (**A,** bottom). (C) Left,

Histograms show the fluorescence intensity of intracellular CD3ζ; right, mean fluorescence intensity (MFI) of intracellular CD3ζ. (D) Representative histogram (left) and MFI (right) of the TCRα/β complex in zBB$^{\Delta BRM}$-transduced CD3ζ-KO Jurkat cells. (E) mRNA expression level of modified-CD3ζ in zBB$^{\Delta BRM}$-transduced CD3ζ-KO Jurkat cells. (F) Amino acid sequences of BB$^{\Delta BRM}$z. (G) Representative histogram (left) and MFI (right) of the TCRα/β complex in BB$^{\Delta BRM}$z-transduced CD3ζ-KO Jurkat cells. (H) Representative histogram (left) and MFI (right) of the TCRα/β complex in zBB$^{K/RtoS}$- or zBB$^{\Delta BRM}$-transduced CD3ζ-KO Jurkat cells. P-values (*P < 0.05, **P < 0.01, ***P < 0.005, and ****P < 0.0001) were determined using one-way ANOVA, with Tukey's multiple comparisons *post-hoc* test (B-E, G, and H). Data have been presented as mean ± SEM. n.s., not significant.

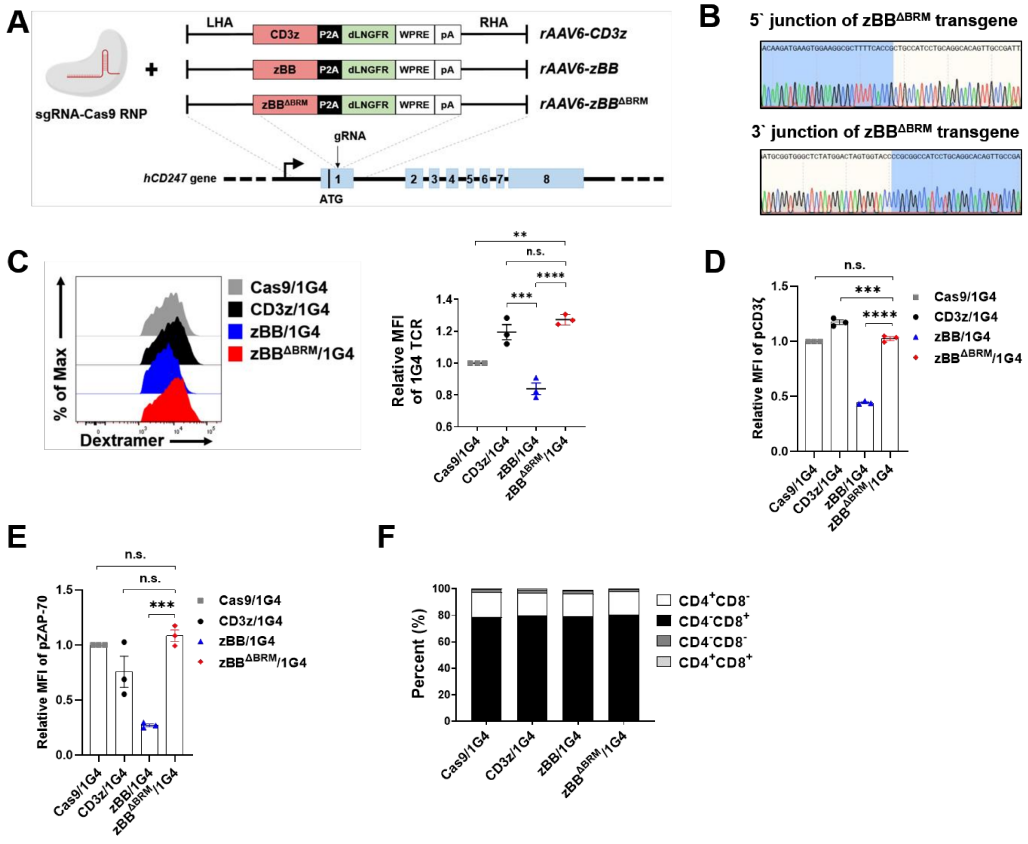

Supplemental figure 9. Generation and analysis of zBB$^{\Delta BRM}$/1G4 T cells.

(A) CRISPR/Cas9-targeted integration of the modified-CD3ζ gene into the *CD247* locus. Top, rAAV6 containing a modified-CD3ζ cassette flanked by homology arms; bottom, *CD247* locus. (B) In-Out PCR for targeted integration of zBB$^{\Delta BRM}$ at *CD247* locus. (C) Surface expression (left) and MFI (right) of the NY-ESO-1-specific TCR (1G4) complex in zBB$^{\Delta BRM}$/1G4 T cells. (D) Phosphorylation of CD3ζ in zBB$^{\Delta BRM}$/1G4 T cells. (E) Phosphorylation of ZAP-70 in zBB$^{\Delta BRM}$/1G4 T cells. (F) CD4/CD8 composition (ratio) in Cas9/1G4, CD3z/1G4, zBB/1G4, and zBB$^{\Delta BRM}$/1G4 T cells. P-values (**P < 0.01, ***P < 0.001, and ****P < 0.0001) were determined using one-way ANOVA, with Tukey's multiple comparisons *post-hoc* test (C-E). Data have been presented as mean ± SEM. n.s., not

147 significant.

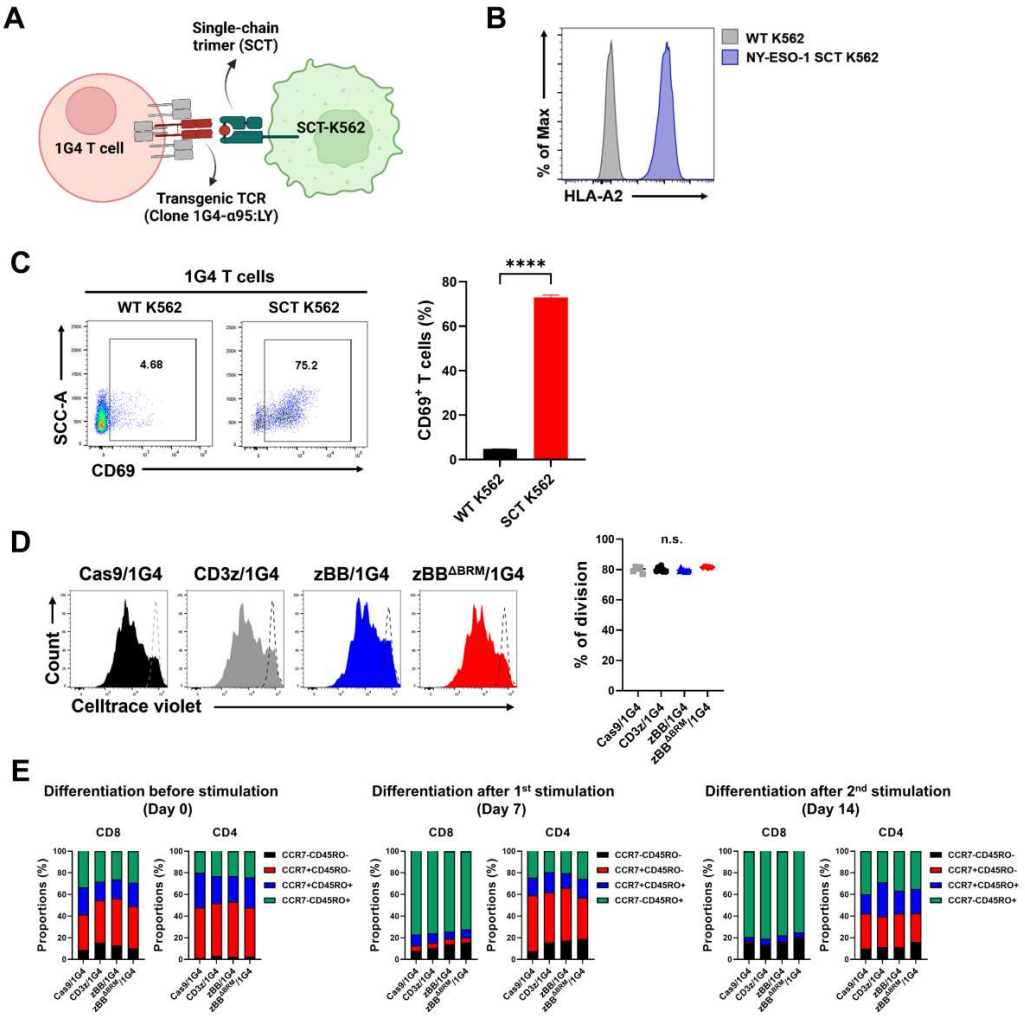

148

149 **Supplemental figure 10. Comparison of 1G4 T cells proliferation in the co-culture with**

150 **SCT-K562 feeder cells.**

151 (A) Schematic diagrams of K562 cell expressing a single-chain trimer (SCT) of HLA-A2

152 linked to the NY-ESO-1 peptide. (B) Representative histograms of HLA-A2 in WT (gray

153 shaded histogram) and NY-ESO-1-SCT (blue shaded histogram) K562 cells. (C) Proportion

154 of the activation marker, CD69, in NY-ESO-1-specific TCR-expressing T cells, after co-

culture with WT or SCT-K562 cells. (D) Representative FACS histogram showing proliferation of CTV-stained 1G4 T cells co-cultured with A375 cells. (E) The differentiation status of CD4+ and CD8+ TCR-T cells were determined by the expression of CCR7 and CD45RO. TCR-T cells were divided into naïve ($CCR7^+CD45RO^-$), central memory ($CCR7^+CD45RO^+$), effector memory ($CCR7^-CD45RO^+$), and terminally differentiated effector ($CCR7^-CD45RO^-$) subpopulations. P-values (****P < 0.0001) were determined using unpaired student's *t*-test (C) and one-way ANOVA, with Tukey's multiple comparisons *post-hoc* test (D). Data have been presented as mean ± SEM. n.s., not significant.

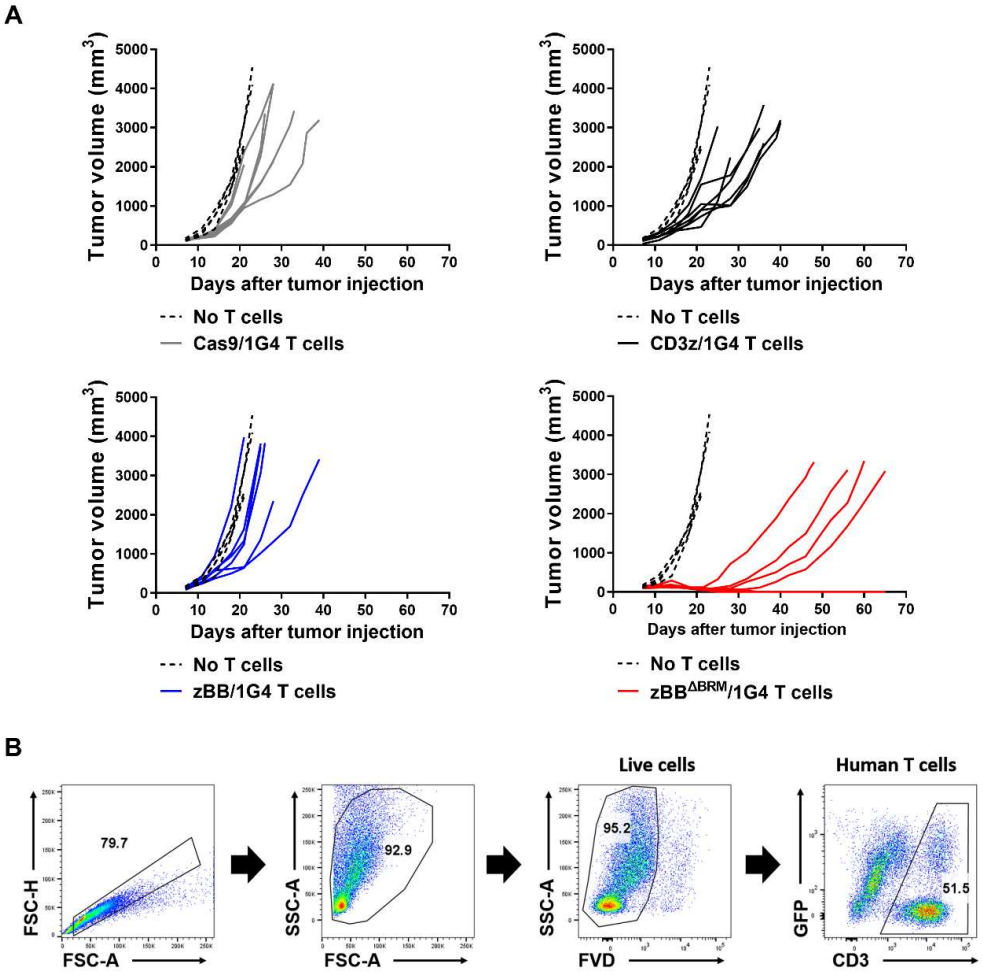

Supplemental figure 11. Individual tumor growth curves and flow cytometry gating strategy for human T cells in tumor.

(A) Individual tumor growth curves for NSG mice injected with A375 melanoma cells and intravenously infused with Cas9/1G4, CD3z/1G4, zBB/1G4, or zBB$^{\Delta BRM}$/1G4 T cells (1×10^6 cells/mouse) when tumors reached ~100 mm^3 (7 days after implantation). Percentages of CRs: control (no T cells), 0% (0/4 mice); Cas9/1G4, 0% (0/7 mice); CD3z/1G4, 0% (0/7 mice); zBB/1G4, 0% (0/6 mice); and zBB$^{\Delta BRM}$/1G4 T cell-infused, 42.9%

(3/7 mice). (B) Flow cytometry gating strategy used to define human T cell populations from A375 melanoma tumor. CR, complete remission; FVD, fixable viability dye; GFP, green fluorescent protein.

Table1. sgRNA targeting *CD247*

sgRNA	Target	sgRNA sequence
#1	*CD247*	GCCTCCCAGCCTCTTTCTGA
#2	*CD247*	AAAGGACAAGATGAAGTGGA
#3	*CD247*	GTGGAAGGCGCTTTTCACCG
#4	*CD247*	CTGTGCCTGCAGGATGGCCG

Supplemental table 1. sgRNA sequences targeting the *CD247* locus.

Supplementary reference

1. Philip B, Kokalaki E, Mekkaoui L, et al. A highly compact epitope-based marker/suicide gene for easier and safer T-cell therapy. *Blood* 2014;124(8):1277-87.